THE JOURNAL OF PHYSICAL CHEMISTRY C

Article

pubs.acs.org/JPCC

One-Pot Epoxide-Driven Synthesis of $M_2Al(OH)_6Cl{\cdot}1.5H_2O$ Layered Double Hydroxides: Precipitation Mechanism and Relative Stabilities

Víctor Oestreicher,[†] Ismael Fábregas,[‡] and Matías Jobbágy*[,†,§]

[†]INQUIMAE-DQIAQF, Facultad de Ciencias Exactas y Naturales, Universidad de Buenos Aires, Ciudad Universitaria, Pab. II, C1428EHA, Buenos Aires, Argentina

[‡]Division of Porous Materials, UNIDEF, CONICET, S.J.B de la Salle 4397, B1603ALO Villa Martelli, Buenos Aires, Argentina

[§]Centro Interdisciplinario de Nanociencia y Nanotecnología, Argentina

Supporting Information

ABSTRACT: A family of single-crystalline particles of $M_2Al(OH)_6Cl{\cdot}1.5H_2O$ layered double hydroxides (LDH) with M(II) a transition-metal cation were obtained by a one-pot room-temperature homogeneous alkalinization driven by glycidol ring opening. In contrast with traditional homogeneous methods, LDH phases are obtained in the exchangeable chloride-containing form. The main precipitation steps were assessed by continuous measurement of pH profiles, field emission scanning electron microscopy, and powder X-ray diffraction, revealing the heterogeneous nucleation of LDH phase over previously formed nano-$Al(OH)_3$ seeds. The precipitation pH plateau of each LDH follows the trend of the inherent solubility of the single M(II) phases obtained under alkalinization. A linear free-energy relation links the solubility of the bare M(II) hydroxides with the correspondent M(II)−Al(III) LDH, in good agreement with previously reported thermochemical models.

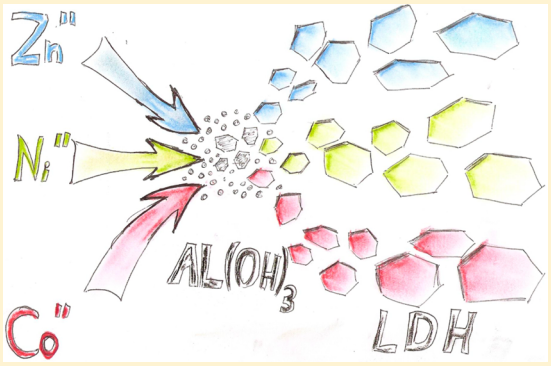

INTRODUCTION

Obtaining carbonate-free single-crystalline layered double hydroxides (LDHs) is a highly desired target in current materials chemistry research. When chloride-containing forms are used as a starting material, nitrate-,[1] perchlorate-, or acetate-containing[2] ones can easily be obtained through anionic exchange.[3−6] These exchanged forms are able to develop massive exfoliation or delamination allowing the preparation of highly oriented self-assembled films,[7] layer-by-layer assemblies, and nanoshells,[8] still preserving their inherent reversible intercalation ability, giving birth to a promising family of advanced materials.[9] Previous attempts to develop these phases by means of a homogeneous alkalinization process partially succeeded by employing the controlled thermal hydrolysis of hexamethylenetetramine (HMT)[10] or formamide[11] while the traditional urea-based methods univocally result in undesired carbonate-bearing LDH phases,[12−17] except for certain Zn(II)−Al(III) phases.[18] To reach exchangeable forms, a time-consuming decarbonation process is mandatory, being particularly tedious for certain LDH phases.[7]

Recently it was demonstrated that Mg(II)−Al(III) LDHs can be obtained through chloride-assisted epoxide ring opening in aqueous solutions at 298 K, a mild method inherently free of carbonated side products.[19] The main process is initiated with the protonation of the oxo bridge with a subsequent nucleophilic attack, commonly driven by chloride, and results in the ring-opening and a net hydroxyl release (eqs S1 and S2 in the Supporting Information).[20]

Additionally, because of the absence of hydrothermal ripening, pristine born single crystals preserving their nanometric thickness can be isolated.

The present study reveals to what extent the aforementioned method allows the one-pot preparation of highly crystalline LDH particles obeying the formula $M_2Al(OH)_6Cl{\cdot}nH_2O$, being M(II) divalent transition-metal cations. Beyond precipitation kinetics, the inherent solubility trend of the obtained phases was analyzed in terms of a general model for LDH stability.

EXPERIMENTAL SECTION

Synthesis. Typically, precipitations were driven by aging for 48 h at 298 K 100 cm^3 of filtered solutions containing NaCl (100−500 mM), glycidol 400 mM, a chloride salt of Co(II), Ni(II), Cu(II) or Zn(II) (6.6−12.0 mM) or a combination of one of the aforementioned divalent cations with Al(III) chloride (2.0−3.3 mM). All reagents were purchased from Sigma-Aldrich and used without further purification. The precipitated solids were collected by centrifugation, washed three times with cold water, and dried at room temperature.

Precipitation pH Profiles. Representative precipitation curves were obtained by in situ potentiometric pH measurement in a reactor at 298 K under permanent stir constantly purged with N_2 to prevent atmospheric CO_2 uptake.

Received: October 14, 2014
Revised: November 29, 2014

   dx.doi.org/10.1021/jp510341q | J. Phys. Chem. C XXXX, XXX, XXX−XXX

Characterization of Solids. All synthesized solids were characterized by powder X-ray diffraction (PXRD) using a graphite-filtered Cu Kα radiation (λ = 1.5406 Å) and a field emission scanning electron microscopy (FESEM) instrument, equipped with an energy dispersive X-ray spectroscopy (EDS) probe. Cation, chloride, and water contents were assessed by ICP, ionic chromatography, and elemental analysis, respectively. *ImageJ* software was employed to analyze the size distribution of obtained particles over 100 particles from each sample. X-ray absorption spectroscopy (XAS) spectra of the samples were acquired in the D04B-XAFS1 beamline[21] of the LNLS, in transmission mode. A Si(111) monochromator for Co−K edge was used. The energy was calibrated with a Co metallic foil. The spectra were taken at room temperature. Three spectra were taken for each sample, and its average used to perform the analysis. To optimize the signal/noise ratio, the thickness of the pellets used for data acquisition was adjusted to obtain a total absorbance above the edge of 1.5.

RESULTS

The inherent precipitation behavior of each M(II) chloride as well as the M(II)−Al(III) binary system was explored. To this aim, precipitation curves for the single M(II) phases and the LDH phases were carried out fixing both glycerol and chloride initial contents according to the previous screening performed over the Mg(II)−Al(III) system.[19] In contrast with Mg(II),[19] all the explored divalent transition cations develop quantitative precipitation in the absence of Al(III) under the employed conditions because of the lower solubility of the correspondent hydroxylated phases. For the sake of clarity, in the following paragraphs the precipitation behavior of each M(II) studied and the correspondent M(II)−Al(III) LDH will be discussed separately before a comprehensive analysis of all the LDH phases obtained. Concerning the epoxide in this study, glycidol was chosen instead of ethylene oxide[22−26] because of its higher boiling point, which makes it easy to handle at room temperature, preventing losses due to evaporation and eventual harmful inhalations.[27]

Precipitation of Co(II) and Co(II)−Al(III) Solutions. Precipitation of Co(II) resulted in a bright green suspension that easily decants. PXRD analysis (Figure 1) denotes the main reflections belonging to a layered hydroxide typically obtained under related conditions, known as α phase.[28] This layered phase bearing the formula $Co^{Oh}_{0.828}Co^{Td}_{0.348}(OH)_2(Cl)_{0.348}\cdot 0.46H_2O$ holds a main fraction of octahedral Co(II) centers, Co^{Oh}, belonging to a hexagonal cationic arrangement. Certain Co^{Oh} positions within each layer are vacant, and these sites are occupied by a couple of tetrahedral Co(II) centers, Co^{Td}, positioned externally from the hydroxilated layer. This structural feature results in an expanded interbasal distance with respect from the brucitic β-$Co(OH)_2$.[29] The green color follows the contribution of the inherent transitions of Co(II) centers present in 4-fold and 6-fold coordination environments. The interbasal distance 003 of 8.04(2) Å and the 110 reflection positioned at 1.572(6) Å recorded for this phase are in good agreement with reported a = 3.1439(5) Å and c = 24.058(6) Å cell parameters.[29] Chemical analysis confirmed a Co(II)-to-chloride ratio of 0.29; FESEM inspection revealed single-crystalline hexagonal platelets ranging from 2 to 12 μm in diameter (Figure 2) and 25(5) nm thick. Once the aforementioned precipitation is performed with a Co(II):Al-(III) 2:1 ratio, a pink colloid consisting of hexagonal platelets was isolated. PXRD of the dry and ground sample (Figure 1) revealed the presence of the main interlamellar 00l reflections of a LDH phase with interbasal distance of 7.8 Å, typically observed for the chloride form of Co(II)−Al(III) LDH.[7,30] As a natural consequence of the thin dimension of the particle along the c direction, broad 00l reflections were observed. The isomorphic substitution of Al(III) within the brucitic planes of $Co(OH)_2$ resulted in a shift of the 110 reflection to 1.534(5) Å, in excellent agreement with reported values for Co(II)−Al(III) LDH phases.[7,31,32] PXRD data as well as the absence of visible light absorption belonging to Co(II) centers in tetrahedral coordination environment, excluded the presence of α-Co(II) hydroxide. XAS-based analysis of cobalt revealed that the absorption edge was essentially at the same energy (7711 eV) as that of Co(II) absorption recorded for reference Co(II)−Al(III) (7712 eV), an LDH phase prepared under well-established protocols (Figure S1 in the Supporting Information).[7] Then, the eventual occurrence of oxidized Co(II)−Co(III) LDH phase was disregarded for Co(II) sample.[33] In the case of the Co(II)−Al(III) sample, the whole spectrum is almost superimposable to the aforementioned LDH reference, confirming the phase purity suggested by PXRD analysis. Both Co(II)−Al(III) and Co(II) sample suspensions revealed liquid crystalline characteristics expected for high aspect ratio platelets.[7] These samples were deposited onto a glass substrate and submitted to controlled evaporation to favor oriented self-assembly of particles. The PXRD recorded for both phases revealed a massive preferential orientation of crystals with their c axis perpendicular to the substrate (Figure 1). The broad reflections recorded suggest a crystalline thickness along the c direction of 25(5) nm, according to Scherrer's equation. For the case of the Co(II)−Al(III) sample, the main reflections can be indexed with the $3R_1$ cell.[34]

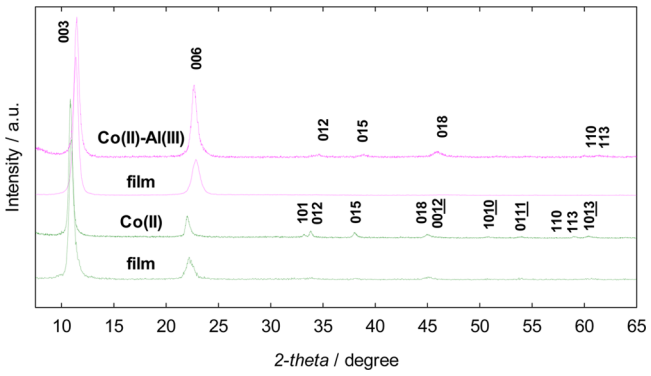

Figure 1. PXRD diffraction of samples obtained from solution containing NaCl 100 mM, glycidol 400 mM, and $CoCl_2$ 6.6 mM (green line) or $CoCl_2$ 6.6 mM and $AlCl_3$ 3.3 mM (pink line), after aging for 48 h at 298 K. The oriented samples of each phase are indicated as *film*.

In contrast with α-Co(II) hydroxide, FESEM inspection (Figure 2) revealed the presence of almost monodispersed particles consisting of 0.5 ± 0.2 μm long hexagonal platelets of a 20 ± 10 nm thickness, in good agreement with PXRD inspection; EDS probe confirmed the coexistence of cobalt, aluminum, and chloride among them.

To gain insights into the precipitation mechanism, pH evolution along the precipitation process was continuously assessed. Figure 3 reflects the pH alkalinization profiles on bare Co(II), Al(III), and Co(II)−Al(III) solutions.[19] Bare Al(III) solution exhibited the first hydroxylation step (step A) with a

dx.doi.org/10.1021/jp510341q | J. Phys. Chem. C XXXX, XXX, XXX−XXX

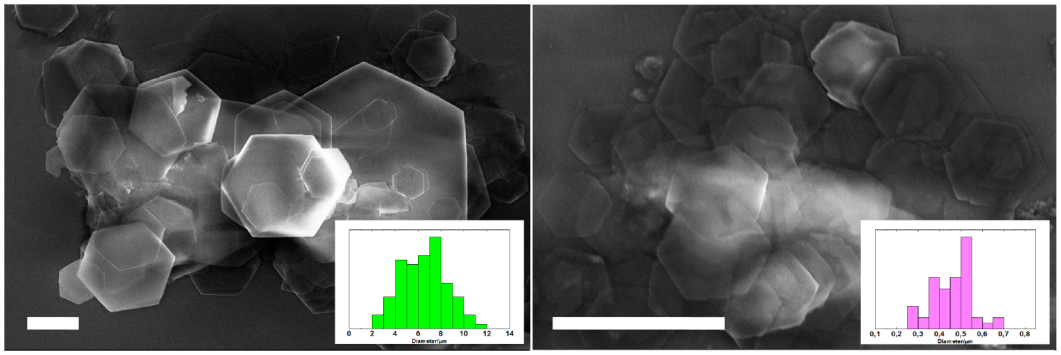

Figure 2. FESEM images of Co(II)−Al(III) particles synthesized from a solution containing NaCl 100 mM, glycidol 400 mM, and $CoCl_2$ 6.6 mM (left panel) or $CoCl_2$ 6.6 mM and $AlCl_3$ 3.3 mM (right panel), aged for 48 h at 298 K. Scale bar represents 2 μm for both images.

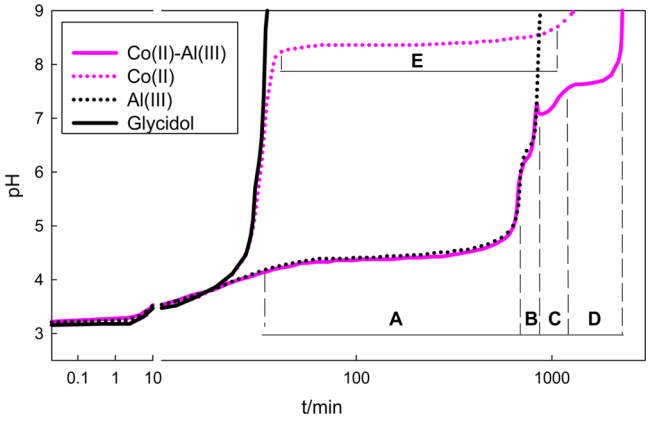

Figure 3. Evolution of pH at 298 K for solution containing NaCl 100 mM, glycidol 400 mM (black line) and $AlCl_3$ 3.3 mM (black dotted line) or $CoCl_2$ 6.6 mM (pink dotted line) or $CoCl_2$ 6.6 mM and $AlCl_3$ 3.3 mM (pink line).

well-defined plateau fixed around pH 4.4, known as the polymerization zone, that obeys OH^- consumption driven by the assembly of Al(III) units into keggin $Al_{13}O_4(OH)_{28}^{3+}$ polycations.[35−38] Then, the translucent stable Al(III) sol coagulates close to pH 6.0, denoting a characteristic second plateau on the alkalinization profile (step B) due to OH^- consumption related to final deprotonation of $Al_{13}O_4(OH)_{28}^{3+}$ polycations. Once this sol flocculates, an ill-crystallized $Al(OH)_3$ phase, characterized by broad PXRD reflections positioned close to Gibbsite or Bayerite ones, is observed.[19,37] When precipitation takes place in the presence of Co(II), the binary solution followed the same behavior, ruled by Al(III) hydrolysis, until step B ends (830 min). Chemical analysis of mother liquors confirmed that this step involved the massive removal of Al(III) ions, exclusively, confirming that its precipitation is totally decoupled from the Co(II) ion precipitation. However, when pH reaches 7.25, it suddenly descends 0.15 units and restores its original value only after 180 min. In principle, this step (step C, Figure 3) of sudden OH^- consumption can obey LDH nucleation and/or specific surface phenomena; because no LDH phase was identified at this stage, the latter phenomena can be ruling the pH profile. Previous reports pointed out that Co(II) develops inner-sphere adsorption onto active $Al(OH)_3$ surface, resulting in a net proton release.[39−45] Additionally, Co(II) adsorption experiments were carried out over bare $Al(OH)_3$ suspensions prepared herein. Independent of the initial amount of Co(II) in the solution, a strong blue color was observed after sorption, indicating the lack of Co^{Oh} in the solids, ruling out the heterogeneous nucleation of LDH onto $Al(OH)_3$ sol particles. In addition, PXRD revealed a pattern almost indistinguishable from that of bare $Al(OH)_3$ phase, confirming the lack of LDH crystallization (Figure S2 in the Supporting Information). Even after a six month aging period of Al(III) sol in contact with Co(II), no sign of the so-called surface precipitation was observed.[46−48]

After spontaneous adsorption, the permanent feed of alkali reverts the pH descent and reaches a critical value around pH 7.6 that triggers a second precipitation event (step D, Figure 3). Massive removal of Co(II) from solution, and the subsequent formation of Co(II)−Al(III) LDH, fixes the pH profile around the value of precipitation, according to eq 1. This process takes place because of the supply of OH^- required to drive the LDH crystallization process, in concordance with related procedures developed regarding γ-Al_2O_3 or nano-AlO(OH).[49,50]

$$2Co^{2+}(aq) + Al(OH)_3(s) + Cl^-(aq) + 3OH^-(aq) + H_2O \rightarrow Co_2Al(OH)_6Cl{\cdot}H_2O(s) \quad (1)$$

As was observed during Mg(II)−Al(III) LDH formation,[19] the freshly precipitated $Al(OH)_3$ nanoparticles are active enough to develop massive dissolution at mild alkaline conditions; the aforementioned precipitation sequence was confirmed for analogous experiments performed under lower alkalinization rates (Figure S3 in the Supporting Information) tuned by different initial chloride and glycidol concentrations.

In contrast with the binary solution, bare Co(II) solution just exhibited a single and well-defined precipitation event (step E, Figure 3), characterized by a plateau fixed around pH 8.2, almost a pH unit over the value recorded for Co(II) precipitation in the presence of Al(III), suggesting the inherently lower solubility (higher stability) of the LDH phase, in accordance with titration-based experiments.[38]

Concerning the mechanism of crystallization, it seems to follow the behavior observed for Mg(II)−Al(III) LDHs prepared under this method. In contrast with previous procedures that report polycrystalline rosettes or central holes among the LDH platelets,[51] their absence suggests that the first LDH nuclei grows onto very small seeds that easily redissolve, preventing the aforementioned textural effects. The observed pH profile is in good agreement with recent reports dealing with the precipitation of Fe(III)-based LDHs.[52]

Precipitation of Ni(II) and Ni(II)−Al(III) Solutions. The precipitation of bare Ni(II) ion solution resulted in a pH profile (Figure S4 in the Supporting Information) analogous to the

dx.doi.org/10.1021/jp510341q | J. Phys. Chem. C XXXX, XXX, XXX−XXX

Co(II) pH profile; a smooth pH overshoot reaching a value of pH 8.5 indicated a nucleation event followed by a precipitation plateau fixed at pH 8.4 inherent to this cation.[53] In contrast, in the presence of Al(III), Ni(II) is incorporated in an LDH phase that precipitates around pH 7.6, well below from the plateau governed by bare Ni(II) phase solubility, confirming the inherent stability of a binary Ni(II)−Al(III) phase. The main features (steps A−D, Figure 3) of the Co(II)−Al(III) precipitation curve are also observed in this case, suggesting the occurrence of an analogous precipitation sequence. For pure Ni(II) phase, PXRD analysis (Figure 4) revealed the

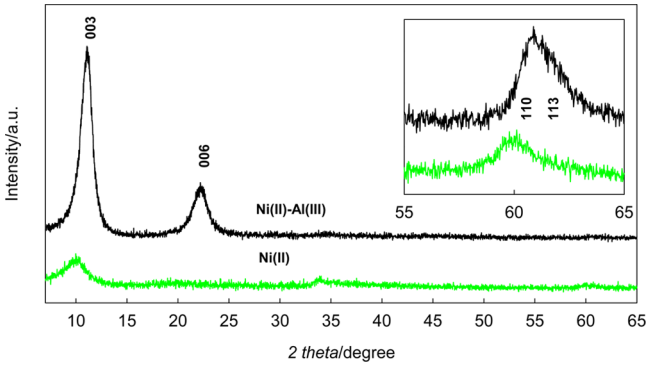

Figure 4. PXRD diffraction of samples obtained after aging for 48 h at 298 K solutions containing NaCl 100 mM, glycidol 400 mM, and $NiCl_2$ 6.6 mM (black line) or $NiCl_2$ 6.6 mM and $AlCl_3$ 3.3 mM (green line).

presence of the main 00*l* reflections of a lamellar hydroxide typically obtained under homogeneous alkalinization conditions, known as α-hydroxide.[53] In contrast with the Co(II) phase, this one consists of a turbostratic lamellar hexagonal phase with octahedral coordinated Ni(II) centers, obeying the formula $Ni(OH)_{2-x}(A)_x \cdot nH_2O$, where A^- represents an exchangeable anion. This phase commonly develops flake-like nanocrystals. As a natural consequence of the thin dimension of the particles, broad 00*l* reflections were observed, which suggests a crystal size along the *c* axis of 6 ± 1 nm. The interbasal distance of 8.8 Å observed for this phase exceeded that of Ni(II)−Al(III), in agreement with previous reports.[30,54,55] The binary Ni(II)−Al(III) precipitated phase revealed the presence of the main reflections of a LDH structure bearing an interlayer distance of 7.98(4) Å and a grain size along the *c* axis of 10 ± 1 nm. The isomorphic substitution of Al(III) within the brucitic planes of $Ni(OH)_2$ resulted in a net shift of the 110 reflection, strongly overlapped with the 113 reflection, to higher angles, in excellent agreement with *a* parameter of 1.592(4) Å, reported for well-crystallized forms of Ni(II)−Al(III) LDHs.[31,56] The lower crystallinity of Ni(II) phases compared to Co(II) obtained herein is a natural result of the lower ability of the former cation to drive ligand exchange process and/or recrystallization.[16]

FESEM images (Figure 5) revealed highly corrugated flakes,[57] as expected for flexible nanometer-thick particles; this characteristic is inherent to high aspect ratio nanoflakes or related compounds with a few unit cells thickness along the *c* direction that eventually can twist around themselves in the form of nanocones.[58]

Precipitation of Zn(II) and Zn(II)−Al(III) Solutions. Bare Zn(II) solution presented a precipitation plateau at pH 7.3 after reaching an overshoot 0.1 units higher (Figure 6). Binary

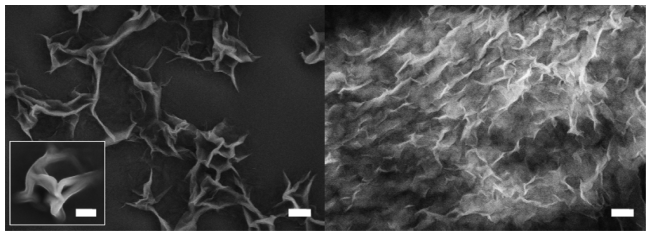

Figure 5. FESEM images of particles synthesized from solution containing NaCl 100 mM, glycidol 400 mM, and $NiCl_2$ 6.6 mM (left panel) or $AlCl_3$ 3.3 mM and $NiCl_2$ 6.6 mM (right panel), aged at 298 K for 48 h. Scale bar represents 200 nm (inset: 100 nm).

Zn(II)−Al(III) solution presented a behavior similar to that of the Co(II)- or Ni(II)-based solutions, with the occurrence of the successive B−D steps.

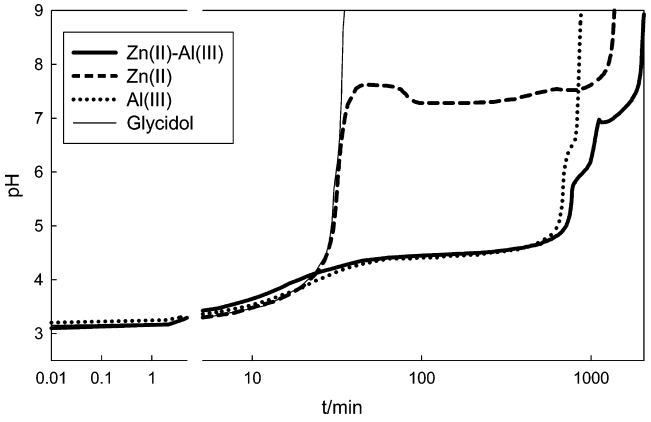

Figure 6. Time evolution of pH at 298 K for solution containing NaCl 100 mM, glycidol 400 mM, and $AlCl_3$ 3.3 mM (dotted line), $ZnCl_2$ 6.6 mM (dashed line), or $ZnCl_2$ 6.6 mM and $AlCl_3$ 3.3 mM (thick solid line). Reference alkalinization curve in the absence of Zn(II) and Al(III) is also presented (thin solid line).

The PXRD pattern of the phase obtained matches with previously observed one for certain layered Zn(II) basic chlorides obtained through anionic exchange under mild conditions from a parent lamellar basic nitrate (Figure 7);[59] no reflections belonging to Simonkolleite ($Zn_5(OH)_8Cl_2 \cdot H_2O$) were observed.[60] The binary Zn(II)−Al(III) system evolved as a stable LDH exhibiting a precipitation pH plateau at 7.08;

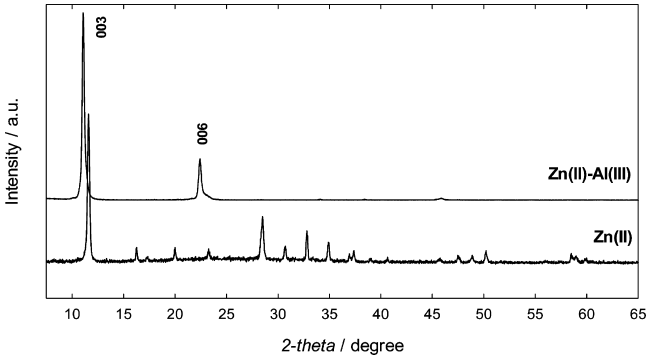

Figure 7. PXRD diffraction of samples obtained after aging for 48 h at 298 K a solution containing NaCl 100 mM, glycidol 400 mM, and $ZnCl_2$ 6.6 mM (lower line) or $ZnCl_2$ 6.6 mM and $AlCl_3$ 3.3 mM (upper line).

dx.doi.org/10.1021/jp510341q | J. Phys. Chem. C XXXX, XXX, XXX−XXX

PXRD inspection revealed a highly crystalline phase that spontaneously develops preferential orientation, as was observed for Co(II)−Al(III) LDH.

FESEM inspection of Zn(II) samples revealed the presence of both mono and polycrystalline hexagonal platelets and rosettes, with well-developed geometric borders and smooth surfaces, suggesting a massive recrystallization (Figure 8).

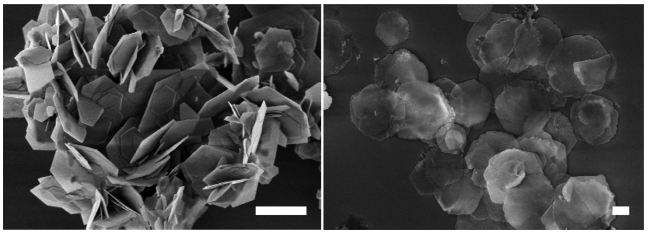

Figure 8. FESEM images of particles synthesized from solution containing NaCl 100 mM, glycidol 400 mM, and $ZnCl_2$ 6.6 mM (left panel) and $ZnCl_2$ 6.6 mM and $AlCl_3$ 3.3 mM (right panel), aged at 298 K for 48 h. Scale bar represents 2 μm for both images.

Almost monodispersed binary Zn(II)−Al(III) particles consisting of 10 ± 3 μm long hexagonal platelets of 50 ± 10 nm thickness; EDS probe confirmed the coexistence of zinc, aluminum, and chloride among them.

Precipitation of Mn(II) and Mn(II)−Al(III) Solutions. The homogeneous alkalinization of either Mn(II) or Mn(II)−Al(III) solutions resulted in the oxidation of Mn(II), excluding the possibility of a permanent pH assessment, even under the constant N_2 bubbling in the reactor. Then, both solutions were precipitated employing Schlenk's device. The resulting white solids immediately exhibit oxidation (brownish color) during centrifugation. However, under PXRD inspection (Figure 9),

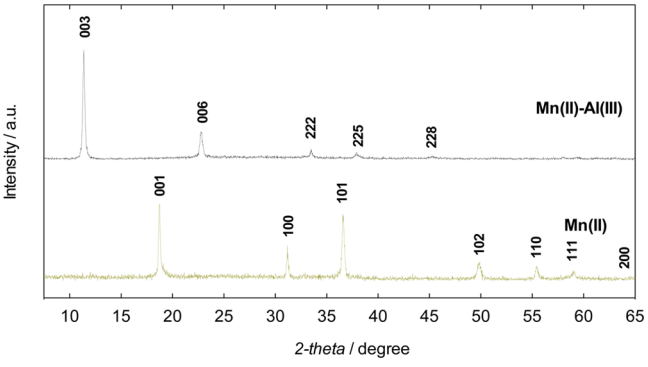

Figure 9. PXRD diffraction patterns of solution containing NaCl 100 mM, glycidol 400 mM, and $MnCl_2$ 6.6 mM (brown line) and $MnCl_2$ 6.6 mM and $AlCl_3$ 3.3 mM (black line), aged at 298 K for 48 h.

both samples evidenced well-crystallized phases that can be indexed as brucitic $Mn(OH)_2$ (c = 4.73 Å, PDF 18-0787) and $Mn_2Al(OH)_6Cl{\cdot}nH_2O$ LDH (c = 7.80 Å, PDF 51-1526), respectively. This behavior is expected in these LDHs; however, in contrast with recent reports,[61] the oxidation products of Mn(II) remain silent to PXRD in both cases, suggesting its occurrence as an ill-crystallized Mn(III) decorating the parent well-crystallized particles. In the former case, no topotactic transformation to $Mn(II)_2Mn(III)(OH)_6Cl{\cdot}nH_2O$ LDH was noticeable.[33]

Precipitation of Cu(II) and Cu(II)−Al(III) Solutions. The exploration of the Cu(II)−Al(III) system revealed a dramatically different behavior. In contrast with the aforementioned cations, Cu(II) bare solution precipitates at around pH 5.5 (Figure 10), in the form of highly crystalline $Cu_2Cl(OH)_3$

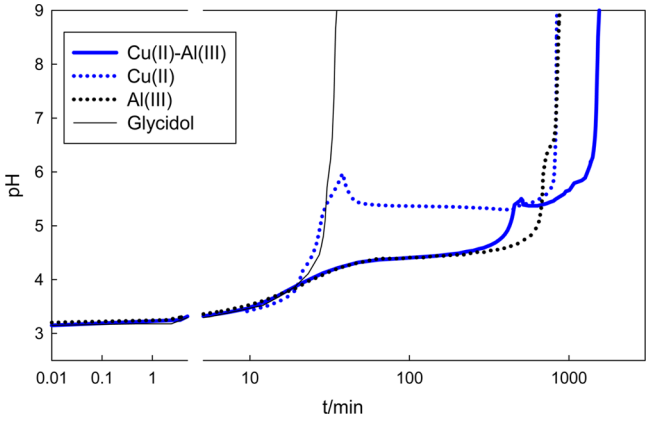

Figure 10. Time evolution of pH at 298 K for solution containing NaCl 100 mM, glycidol 400 mM (black line), and $AlCl_3$ 3.3 mM (black dotted line), $CuCl_2$ 6.6 mM (blue dotted line) or $CuCl_2$ 6.6 mM and $AlCl_3$ 3.3 mM (blue line).

(clinoatacamite, PDF 50-1559; Figure S6 in the Supporting Information) particles. Moreover, the inherent pH of the precipitation's plateau remains undisturbed in the presence of $Al(OH)_3$ nanoparticles, except for a lower pH overshoot. The $Cu_2Cl(OH)_3$ phase remains as the only Cu(II) crystalline product without any evidence of LDH phase crystallization. This is expected because previous experimental reports[62] as well as in silico calculations predict intrinsic lower stability for the Cu(II)−Al(III) LDH structure with respect to the other M(II)−Al(III) forms.[63] The origin of this peculiar behavior probably lies in the inherent distorted coordination environment that d^9 Cu(II) ions tend to adopt, even for the bare $Cu(OH)_2$ orthorhombic phase, that results in a low solubility (Table 1). Beyond thermodynamic aspects, the presence of

Table 1. Solubility Constants of M(II) Hydroxides or Basic Chlorides and Their Correspondent $M_2Al(OH)_6Cl$ LDH Phases

cation	phase	pK_{sp}	pK_{sp} $M_2Al(OH)_6Cl$
Al(III)	$Al(OH)_3$ (from ref 19)	31.75 ± 0.25	–
Mg(II)	$Mg(OH)_2$ (from ref 19)	9.9 ± 0.15	50.5 ± 0.35
Co(II)	$Co(OH)_{1.4}Cl_{0.6}{\cdot}nH_2O$	11.2 ± 0.15	57.10 ± 0.35
Ni(II)	$Ni(OH)_{1.5}Cl_{0.5}{\cdot}nH_2O$	11.4 ± 0.15	56.95 ± 0.35
Zn(II)	$Zn(OH)_{1.6}Cl_{0.4}{\cdot}nH_2O$	13.6 ± 0.15	58.5 ± 0.35
Cu(II)	$Cu(OH)_{1.5}Cl_{0.5}$	15.7 ± 0.15	–

$Al(OH)_3$ nanoparticles affected the texture of $Cu_2Cl(OH)_3$ phase that resulted in much smaller crystals, suggesting that the former phase acts as nucleation seed for the latter (Figure S5 in the Supporting Information). To favor the LDH precipitation phase, different precipitation conditions were tested. Alkalinization rate can be modulated both by initial glycidol or chloride concentration; slower precipitation rates were evaluated, to favor the precipitation of thermodynamically stable phases. However, the segregation of $Cu_2Cl(OH)_3$ prevails over the LDH phase in all the cases.

dx.doi.org/10.1021/jp510341q | J. Phys. Chem. C XXXX, XXX, XXX−XXX

DISCUSSION

Because of the mild alkalinization rate employed, a permanent solubility equilibrium condition for the solid phases growing along the precipitation plateau can be assumed; the formula that describes solubility equilibrium of growing LDH is $M(II)_2Al(OH)_6Cl{\cdot}1.5H_2O$, the stable M(II)-to-Al(III) ratio typically observed.[64]

The occurrence of certain Al(III)-rich LDH phases obeying the formula $MAl_4(OH)_{12}(NO_3)_2{\cdot}nH_2O$, with M(II) = Co(II), Ni(II), Cu(II), Zn(II) as alternative phases to the observed LDHs was expectable. Interestingly, this intercalation process takes place without the addition of extra base, when solutions of these cations are exposed to the proper $Al(OH)_3$ phase under hydrothermal conditions according to eq 2.[65]

$$M^{2+}(aq) + 2Cl^-(aq) + 4Al(OH)_3(s) + nH_2O(1) \rightarrow MAl_4(OH)_{12}Cl_2{\cdot}nH_2O(s) \quad (2)$$

However, the mild conditions employed herein seem to prevent this from happening, and only the OH^- supply allows the crystallization of the $Co_2Al(OH)_6Cl{\cdot}H_2O$ phase.

Before LDH nucleation, the concentration of free Al(III) ions is fixed by the solubility equilibria of already precipitated $Al(OH)_3$. Assuming that this equilibrium is valid until the parent $Al(OH)_3$ sol is consumed, each one of the M(II) precipitation plateaus allows an estimation of the solubility of their correspondent M(II)−Al(III) LDH phases. Table 1 compiles those LDH pK_{sp} values as well as the inherent pK_{sp} value for the bare M(II) basic chlorides obtained under similar conditions. For the particular case of Mg(II)−Al(III) phase, the deduced value is in excellent agreement with the solubility data recorded for this phase under complementary dissolution experiments.[66]

In recent years, several authors postulated that the thermodynamic stability of a given LDH phase is governed by the inherent one of the pure hydroxides of the constituent cations.[67−69] To test this hypothesis, the present LDH solubility data as well as previously reported result[38] was contrasted against reference solubility values for the pure brucitic hydroxides of the constituent M(II) cations evaluated herein. Figure 11 compiles LDH solubility as a function of $M(OH)_2$ solubility data from different reference sources, expressed in a logarithmic form proportional to dissolution free energy. It is worth mentioning that both sets of LDH solubility data were assessed under different protocols, in terms of both precipitation driving force (cations concentration) and base addition; their coincident values suggest that the assumption of solubility equilibrium condition is valid for both. Despite certain dispersion arising from discrepancies of tabulated values, a robust, almost linear tendency can be observed.

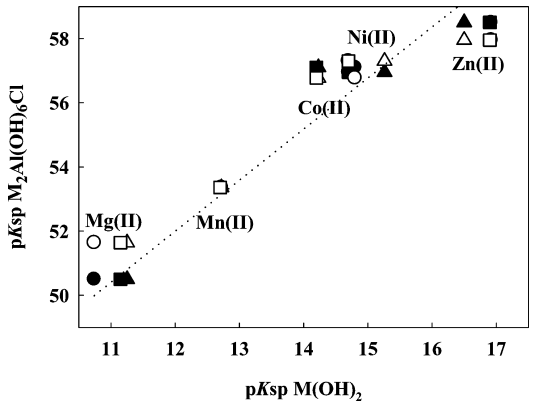

Figure 11. Experimental solubility product (filled symbols) and values reported in ref 38 (empty symbols) as a function of tabulated M(II) solubility product from ref 70 (circles), ref 71 (triangles), and ref 72 (squares).

Interestingly, it predicts that the solubility of an LDH phase constituted by Al(III) and an extremely soluble hypothetical M(II) cation is practically that of $Al(OH)_3$ itself. Then, the slope value of 1.6 of this tendency indicates that the linear free-energy relation that links the solubility of the bare hydroxides with the M(II)−Al(III) LDH one can be resumed in the form of eq 3.

$$K_{sp}\{Al(OH)_3\} + 1.6K_{sp}\{M(OH)_2\} = K_{sp}\{MAl(OH)_6Cl{\cdot}H_2O\} \quad (3)$$

CONCLUSIONS

The present study demonstrates that it is possible to obtain a variety of single-crystalline particles of Al(III)-based LDH in the exchangeable chloride form by means of a mild homogeneous alkalinization procedure based on chloride-assisted glycidol ring rupture. Certain LDH phases such as Mn(II)−Al(III) LDH that cannot be obtained by ammonia-releasing agents were obtained in the present case.[31] The in situ measurement of pH profiles allowed us to observe the main precipitation steps already observed for Mg(II)−Al(III) LDH. The heterogeneous nucleation of LDH phase over existing nano-$Al(OH)_3$ seeds is preceded by surface adsorption of M(II) ions onto them; once the LDH phase nucleates, its growth is driven by M(II) and OH^- consumption from solution as well as massive redissolution of the nano-$Al(OH)_3$ particles. The precipitation pH plateau of each LDH follows the trend of the solubility of the hydroxichlorides obtained under similar conditions as well as the tabulated solubility of bare M(II) hydroxides. For the particular case of Cu(II), the inherent stability of the basic chloride hinders the growth of the Cu(II)−Al(III) LDH phase. The extension of the present method for the obtainment of LDH phases holding higher M(II)-to-Al(III) ratios and/or different interlayer anions is under current research.

ASSOCIATED CONTENT

Supporting Information

XANES spectra, PXRD patterns, and time evolution of pH and FESEM images. This material is available free of charge via the Internet at http://pubs.acs.org.

AUTHOR INFORMATION

Corresponding Author

*E-mail: jobbag@qi.fcen.uba.ar. Fax: 54-11-45763341.

Notes

The authors declare no competing financial interest.

ACKNOWLEDGMENTS

This work was supported by the University of Buenos Aires (UBACyT 20020130100610BA), the Agencia Nacional de Promoción Científica y Tecnológica (ANPCyT PICT 2012-1167), the National Research Council of Argentina (CONICET PIP 11220110101020), and the Brazilian Synchrotron

Light Laboratory (LNLS) under proposal D04B-XAFS1 # 10135. V.O. acknowledges CONICET for doctoral fellowship and A.L.N. for daily support. I.F. and M.J. are Research Scientists of CONICET.

REFERENCES

(1) Liu, Z.; Ma, R.; Ebina, Y.; Iyi, N.; Takada, K.; Sasaki, T. General Synthesis and Delamination of Highly Crystalline Transition-Metal-Bearing Layered Double Hydroxides. *Langmuir* **2007**, *23*, 861−867.
(2) Iyi, N.; Ebina, Y.; Sasaki, T. Water-Swellable MgAl-LDH (Layered Double Hydroxide) Hybrids: Synthesis, Characterization, and Film Preparation. *Langmuir* **2008**, *24*, 5591−5598.
(3) Miyata, S. Anion-Exchange Properties of Hydrotalcite-Like Compounds. *Clays Clay Miner.* **1983**, *31*, 305−311.
(4) Jobbágy, M.; Regazzoni, A. E. Anion-Exchange Equilibrium and Phase Segregation in Hydrotalcite Systems: Intercalation of Hexacyanoferrate(III) Ions. *J. Phys. Chem. B* **2005**, *109*, 389−393.
(5) Oestreicher, V.; Jobbágy, M.; Regazzoni, A. E. Halide Exchange on Mg(II)-Al(III) Layered Double Hydroxides: Exploring Affinities and Electrostatic Predictive Models. *Langmuir* **2014**, *30*, 8408−8415.
(6) Costantino, U.; Vivani, R.; Bastianini, M.; Costantino, F.; Nocchetti, M. Ion Exchange and Intercalation Properties of Layered Double Hydroxides Towards Halide Anions. *Dalton Trans.* **2014**, *43*, 11587−11596.
(7) Liu, Z. P.; Ma, R. Z.; Osada, M.; Iyi, N.; Ebina, Y.; Takada, K.; Sasaki, T. Synthesis, Anion Exchange, and Delamination of Co-Al Layered Double Hydroxide: Assembly of the Exfoliated Nanosheet/Polyanion Composite Films and Magneto-Optical Studies. *J. Am. Chem. Soc.* **2006**, *128*, 4872−4880.
(8) Li, L.; Ma, R. Z.; Iyi, N.; Ebina, Y.; Takada, K.; Sasaki, T. Hollow Nanoshell of Layered Double Hydroxide. *Chem. Commun. (Cambridge, U.K.)* **2006**, 3125−3127.
(9) Wang, Q.; O'Hare, D. Recent Advances in the Synthesis and Application of Layered Double Hydroxide (LDH) Nanosheets. *Chem. Rev. (Washington, DC, U.S.)* **2012**, *112*, 4124−4155.
(10) Antonyraj, C. A.; Koilraj, P.; Kannan, S. Synthesis of Delaminated LDH: A Facile Two Step Approach. *Chem. Commun. (Cambridge, U.K.)* **2010**, *46*, 1902−1904.
(11) Manohara, G. V.; Kunz, D. A.; Kamath, P. V.; Milius, W.; Breu, J. Homogeneous Precipitation by Formamide Hydrolysis: Synthesis, Reversible Hydration, and Aqueous Exfoliation of the Layered Double Hydroxide (LDH) of Ni and Al. *Langmuir* **2010**, *26*, 15586−15591.
(12) Cai, H.; Hillier, A. C.; Franklin, K. R.; Nunn, C. C.; Ward, M. D. Nanoscale Imaging of Molecular Adsorption. *Science* **1994**, *266*, 1551−1555.
(13) Costantino, U.; Marmottini, F.; Nocchetti, M.; Vivani, R. New Synthetic Routes to Hydrotalcite-Like Compounds. Characterisation and Properties of the Obtained Materials. *Eur. J. Inorg. Chem.* **1998**, 1439−1446.
(14) Ogawa, M.; Kaiho, H. Homogeneous Precipitation of Uniform Hydrotalcite Particles. *Langmuir* **2002**, *18*, 4240−4242.
(15) Benito, P.; Herrero, M.; Barriga, C.; Labajos, F. M.; Rives, V. Microwave-Assisted Homogeneous Precipitation of Hydrotalcites by Urea Hydrolysis. *Inorg. Chem.* **2008**, *47*, 5453−5463.
(16) Jobbágy, M.; Blesa, M. A.; Regazzoni, A. E. Homogeneous Precipitation of Layered Ni(II)-Cr(III) Double Hydroxides. *J. Colloid Interface Sci.* **2007**, *309*, 72−77.
(17) Oh, J. M.; Hwang, S. H.; Choy, J. H. The Effect of Synthetic Conditions on Tailoring the Size of Hydrotalcite Particles. *Solid State Ionics* **2002**, *151*, 285−291.
(18) Inayat, A.; Klumpp, M.; Schwieger, W. The Urea Method for the Direct Synthesis of ZnAl Layered Double Hydroxides with Nitrate as the Interlayer Anion. *Appl. Clay Sci.* **2011**, *51*, 452−459.
(19) Oestreicher, V.; Jobbágy, M. One Pot Synthesis of $Mg_2Al(OH)_6Cl{\cdot}1.5H_2O$ Layered Double Hydroxides: The Epoxide Route. *Langmuir* **2013**, *29*, 12104−12109.
(20) Brönsted, J. N.; Kilpatrick, M.; Kilpatrick, M. Kinetic Studies on Ethylene Oxides. *J. Am. Chem. Soc.* **1929**, *51*, 428−461.
(21) Tolentino, H.; Cezar, J. C.; Cruz, D. Z.; Compagnon-Cailhol, V.; Tamura, E.; Alves, M. C. M. Commissioning and First Results of the LNLS XAFS Beamline. *J. Synchrotron Radiat.* **1998**, *5*, 521−523.
(22) Gash, A. E.; Tillotson, T. M.; Satcher, J. H.; Poco, J. F.; Hrubesh, L. W.; Simpson, R. L. Use of Epoxides in the Sol-Gel Synthesis of Porous Iron(III) Oxide Monoliths from Fe(III) Salts. *Chem. Mater.* **2001**, *13*, 999−1007.
(23) Gash, A. E.; Tillotson, T. M.; Satcher, J. H.; Hrubesh, L. W.; Simpson, R. L. New Sol-Gel Synthetic Route to Transition and Main-Group Metal Oxide Aerogels Using Inorganic Salt Precursors. *J. Non-Cryst. Solids* **2001**, *285*, 22−28.
(24) Gash, A. E.; Satcher, J. H.; Simpson, R. L. Monolithic Nickel(II)-Based Aerogels Using an Organic Epoxide: The Importance of the Counterion. *J. Non-Cryst. Solids* **2004**, *350*, 145−151.
(25) Gash, A. E.; Satcher, J. H.; Simpson, R. L. Strong Akaganeite Aerogel Monoliths Using Epoxides: Synthesis and Characterization. *Chem. Mater.* **2003**, *15*, 3268−3275.
(26) Zhang, H. D.; Li, B.; Zheng, Q. X.; Jiang, M. H.; Tao, X. T. Synthesis and Characterization of Monolithic Gd_2O_3 Aerogels. *J. Non-Cryst. Solids* **2008**, *354*, 4089−4093.
(27) Ehrenberg, L.; Hussain, S. Genetic Toxicity of Some Important Epoxides. *Mutat. Res.* **1981**, *86*, 1−113.
(28) Cui, H. T.; Zhao, Y. N.; Ren, W. Z.; Wang, M. M.; Liu, Y. Large Scale Selective Synthesis of α-$Co(OH)_2$ and β-$Co(OH)_2$ Nanosheets through a Fluoride Ions Mediated Phase Transformation Process. *J. Alloys Compd.* **2013**, *562*, 33−37.
(29) Ma, R. Z.; Liu, Z. P.; Takada, K.; Fukuda, K.; Ebina, Y.; Bando, Y.; Sasaki, T. Tetrahedral Co(II) Coordination in α-Type Cobalt Hydroxide: Rietveld Refinement and X-Ray Absorption Spectroscopy. *Inorg. Chem.* **2006**, *45*, 3964−3969.
(30) Leroux, F.; Moujahid, E.; Taviot-Gueho, C.; Besse, J. P. Effect of Layer Charge Modification for Co-A1 Layered Double Hydroxides: Study by X-Ray Absorption Spectroscopy. *Solid State Sci.* **2001**, *3*, 81−92.
(31) Johnsen, R. E.; Krumeich, F.; Norby, P. Structural and Microstructural Changes During Anion Exchange of CoAl Layered Double Hydroxides: An In Situ X-Ray Powder Diffraction Study. *J. Appl. Crystallogr.* **2010**, *43*, 434−447.
(32) Richardson, I. G. Zn- and Co-Based Layered Double Hydroxides: Prediction of the a Parameter from the Fraction of Trivalent Cations and Vice Versa. *Acta Crystallogr., Sect. B: Struct. Sci.* **2013**, *69*, 414−417.
(33) Ma, R.; Takada, K.; Fukuda, K.; Iyi, N.; Bando, Y.; Sasaki, T. Phase Transitions - Topochemical Synthesis of Monometallic (Co^{2+}-Co^{3+}) Layered Double Hydroxide and Its Exfoliation into Positively Charged $Co(OH)_2$ Nanosheets. *Angew. Chem., Int. Ed.* **2008**, *47*, 86−89.
(34) Radha, S.; Kamath, P. V. Structural Synthon Approach to Predict the Possible Polytypes of Layered Double Hydroxides. *Z. Anorg. Allg. Chem.* **2012**, *638*, 2317−2323.
(35) Bi, S. P.; Wang, C. Y.; Cao, Q.; Zhang, C. H. Studies on the Mechanism of Hydrolysis and Polymerization of Aluminum Salts in Aqueous Solution: Correlations between The "Core-Links" Model and "Cage-Like" Keggin-Al-13 Model. *Coord. Chem. Rev.* **2004**, *248*, 441−455.
(36) Vermeulen, A. C.; Geus, J. W.; Stol, R. J.; Debruyn, P. L. Hydrolysis-Precipitation Studies of Aluminum (III) Solutions 0.1. Titration of Acidified Aluminum Nitrate Solutions. *J. Colloid Interface Sci.* **1975**, *51*, 449−458.
(37) Stol, R. J.; Vanhelden, A. K.; De Bruyn, P. L. Hydrolysis-Precipitation Studies of Aluminum (III) Solutions 0.2. Kinetic Study and Model. *J. Colloid Interface Sci.* **1976**, *57*, 115−131.
(38) Boclair, J. W.; Braterman, P. S. Layered Double Hydroxide Stability. 1. Relative Stabilities of Layered Double Hydroxides and Their Simple Counterparts. *Chem. Mater.* **1999**, *11*, 298−302.
(39) Parks, G. A. The Isoelectric Points of Solid Oxides, Solid Hydroxides, and Aqueous Hydroxo Complex Systems. *Chem. Rev. (Washington, DC, U.S.)* **1965**, *65*, 177−198.

(40) Hiemstra, T.; Yong, H.; Van Riemsdijk, W. H. Interfacial Charging Phenomena of Aluminum (Hydr)Oxides. *Langmuir* **1999**, *15*, 5942−5955.
(41) Kosmulski, M. pH-dependent Surface Charging and Points of Zero Charge III. Update. *J. Colloid Interface Sci.* **2006**, *298*, 730−741.
(42) Kosmulski, M.; Plak, A. Surface Charge of Anatase and Alumina in Mixed Solvents. *Colloids Surf., A* **1999**, *149*, 409−412.
(43) Vakros, J.; Bourikas, K.; Perlepes, S.; Kordulis, C.; Lycourghiotis, A. Adsorption of Cobalt Ions on The "Electrolytic Solution/γ-Alumina" Interface Studied by Diffuse Reflectance Spectroscopy (DRS). *Langmuir* **2004**, *20*, 10542−10550.
(44) Ataloglou, T.; Bourikas, K.; Vakros, J.; Kordulis, C.; Lycourghiotis, A. Kinetics of Adsorption of the Cobalt Ions on The "Electrolytic Solution/γ-Alumina" Interface. *J. Phys. Chem. B* **2005**, *109*, 4599−4607.
(45) Spanos, N.; Lycourghiotis, A. Mechanism of Deposition of Co^{2+} and Ni^{2+} Ions on the Interface between Pure and F-Doped γ-Alumina and the Impregnating Solution. *J. Chem. Soc., Faraday Trans.* **1993**, *89*, 4101−4107.
(46) Scheidegger, A. M.; Lamble, G. M.; Sparks, D. L. Spectroscopic Evidence for the Formation of Mixed-Cation Hydroxide Phases Upon Metal Sorption on Clays and Aluminum Oxides. *J. Colloid Interface Sci.* **1997**, *186*, 118−128.
(47) d'Espinose De La Caillerie, J. B.; Kermarec, M.; Clause, O. Impregnation of γ-Alumina with Ni(II) or Co(II) Ions at Neutral pH: Hydrotalcite-Type Coprecipitate Formation and Characterization. *J. Am. Chem. Soc.* **1995**, *117*, 11471−11481.
(48) d'Espinose De La Caillerie, J. B.; Clause, O. Promotion of γ-Alumina Dissolution by Metal Ions During Impregnation. Thermal Stability of the Formed Coprecipitates. *Stud. Surf. Sci. Catal.* **1996**, *101*, 1321−1330.
(49) Xu, R.; Zeng, H. C. Synthesis of Nanosize Supported Hydrotalcite-Like Compounds $CoAl_x(OH)_{2+2x}(CO_3)_y(NO_3)_{x-2y}\cdot nH_2O$ on γ-Al_2O_3. *Chem. Mater.* **2001**, *13*, 297−303.
(50) Yang, Y.; Zhao, X.; Zhu, Y.; Zhang, F. Transformation Mechanism of Magnesium and Aluminum Precursor Solution into Crystallites of Layered Double Hydroxide. *Chem. Mater.* **2012**, *24*, 81−87.
(51) Okamoto, K.; Iyi, N.; Sasaki, T. Factors Affecting the Crystal Size of the MgAl-LDH (Layered Double Hydroxide) Prepared by Using Ammonia-Releasing Reagents. *Appl. Clay Sci.* **2007**, *37*, 23−31.
(52) Gregoire, B.; Ruby, C.; Carteret, C. Hydrolysis of Mixed Ni^{2+}-Fe^{3+} and Mg^{2+}-Fe^{3+} Solutions and Mechanism of Formation of Layered Double Hydroxides. *Dalton Trans.* **2013**, *42*, 15687−15698.
(53) Soler-Illia, G.; Jobbágy, M.; Regazzoni, A. E.; Blesa, M. A. Synthesis of Nickel Hydroxide by Homogeneous Alkalinization. Precipitation Mechanism. *Chem. Mater.* **1999**, *11*, 3140−3146.
(54) Delahaye-Vidal, A.; Beaudoin, B.; Sac-Epee, N.; Tekaia-Elhsissen, K.; Audemer, A.; Figlarz, M. Structural and Textural Investigations of the Nickel Hydroxide Electrode. *Solid State Ionics* **1996**, *84*, 239−248.
(55) Oliva, P.; Leonardi, J.; Laurent, J. F.; Delmas, C.; Braconnier, J. J.; Figlarz, M.; Fievet, F.; Deguibert, A. Review of the Structure and the Electrochemistry of Nickel Hydroxides and Oxy-Hydroxides. *J. Power Sources* **1982**, *8*, 229−255.
(56) Richardson, I. G. The Importance of Proper Crystal-Chemical and Geometrical Reasoning Demonstrated Using Layered Single and Double Hydroxides. *Acta Crystallogr., Sect. B: Struct. Sci.* **2013**, *69*, 150−162.
(57) Li, H. B.; Yu, M. H.; Wang, F. X.; Liu, P.; Liang, Y.; Xiao, J.; Wang, C. X.; Tong, Y. X.; Yang, G. W. Amorphous Nickel Hydroxide Nanospheres with Ultrahigh Capacitance and Energy Density as Electrochemical Pseudocapacitor Materials. *Nat. Commun.* **2013**, *4*, No. 10.1038/ncomms2932.
(58) Liu, X. H.; Ma, R. Z.; Bando, Y.; Sasaki, T. A General Strategy to Layered Transition-Metal Hydroxide Nanocones: Tuning the Composition for High Electrochemical Performance. *Adv. Mater. (Weinheim, Ger.)* **2012**, *24*, 2148−2153.
(59) Thomas, N.; Rajamathi, M. Near 100% Selectivity in Anion Exchange Reactions of Layered Zinc Hydroxy Nitrate. *J. Colloid Interface Sci.* **2011**, *362*, 493−496.
(60) Tanaka, H.; Fujioka, A.; Futoyu, A.; Kandori, K.; Ishikawa, T. Synthesis and Characterization of Layered Zinc Hydroxychlorides. *J. Solid State Chem.* **2007**, *180*, 2061−2066.
(61) Abellan, G.; Carrasco, J. A.; Coronado, E. Room Temperature Magnetism in Layered Double Hydroxides Due to Magnetic Nanoparticles. *Inorg. Chem.* **2013**, *52*, 7828−7830.
(62) Alejandre, A.; Medina, F.; Salagre, P.; Correig, X.; Sueiras, J. E. Preparation and Study of Cu-Al Mixed Oxides Via Hydrotalcite-Like Precursors. *Chem. Mater.* **1999**, *11*, 939−948.
(63) Yan, H.; Wei, M.; Ma, J.; Li, F.; Evans, D. G.; Duan, X. Theoretical Study on the Structural Properties and Relative Stability of M(II)-Al Layered Double Hydroxides Based on a Cluster Model. *J. Phys. Chem. A* **2009**, *113*, 6133−6141.
(64) Hibino, T.; Ohya, H. Synthesis of Crystalline Layered Double Hydroxides: Precipitation by Using Urea Hydrolysis and Subsequent Hydrothermal Reactions in Aqueous Solutions. *Appl. Clay Sci.* **2009**, *45*, 123−132.
(65) Fogg, A. M.; Williams, G. R.; Chester, R.; O'Hare, D. A Novel Family of Layered Double Hydroxides - $MAl_4(OH)_{12}(NO_3)_2\cdot H_2O$ (M = Co, Ni, Cu, Zn). *J. Mater. Chem.* **2004**, *14*, 2369−2371.
(66) Jobbágy, M.; Regazzoni, A. E. Dissolution of Nano-Size Mg-Al-Cl Hydrotalcite in Aqueous Media. *Appl. Clay Sci.* **2011**, *51*, 366−369.
(67) Allada, R. K.; Navrotsky, A.; Berbeco, H. T.; Casey, W. H. Thermochemistry and Aqueous Solubilities of Hydrotalcite-Like Solids. *Science* **2002**, *296*, 721−723.
(68) Bravo-Suárez, J. J.; Páez-Mozo, E. A.; Oyama, S. T. Models for the Estimation of Thermodynamic Properties of Layered Double Hydroxides: Application to the Study of Their Anion Exchange Characteristics. *Quim. Nova* **2004**, *27*, 574−581.
(69) Bravo-Suarez, J. J.; Paez-Mozo, E. A.; Oyama, S. T. Review of the Synthesis of Layered Double Hydroxides: A Thermodynamic Approach. *Quim. Nova* **2004**, *27*, 601−614.
(70) *Dean's Analytical Chemistry Handbook*, 2nd ed.; McGraw-Hill: New York, 2004.
(71) *Lange's Handbook of Chemistry*; McGraw-Hill: New York, 1998.
(72) Baes, C. F. J.; Mesmer, R. E. *The Hydrolysis of Cations*; Wiley: New York, 1976.